

# Rotating Disk Electrode Voltammetry Applied to the Kinetics of Uptake and Efflux in Wild-Type and Mutant Catecholamine Transporters

Kristina S. Danek Burgess, Joseph W. Kable, and Joseph B. Justice, Jr.\*

Department of Chemistry, Emory University, Atlanta, Georgia, USA

Received: October 14, 1998

Final version: January 12, 1999

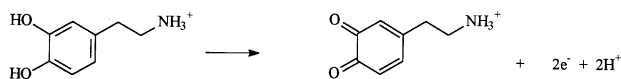
## Abstract

Rotating disk electrode voltammetry has shown to be a simple, fast, and inexpensive method for studying substrate kinetics at wild-type and mutant catecholamine transporters. The transport of the substrates dopamine (DA) and *meta*- and *para*-tyramine (*m*-TYR, *p*-TYR) are examined at the human norepinephrine transporter (hNET) expressed stably in LLC cells. Following uptake of DA, monitored at 450 mV (vs. Ag/AgCl), efflux is induced by the uptake of a second substrate. The timecourse of induced efflux of DA is found to be dependent on the structure of the compound used to initiate efflux as well as the concentration of both the preloaded substrate and efflux inducing agent. A double electrode configuration for the electrochemical cell, including one rotating and one stationary working electrode, is described. A potential of 650 mV is applied across the stationary electrode to obtain the timecourse of single-hydroxyl substrates after correction for any catechol substrate oxidation. This dual electrode set-up is useful in that it allows the kinetics of two substrates interacting at the transporter to be monitored simultaneously. The kinetics of the above mentioned substrates are examined at wild-type and mutant hNETs using this two electrode configuration

**Keywords:** Voltammetry, Transporter, Dopamine, Tyramine, Kinetics

## 1. Introduction

Rotating disk electrode voltammetry (RDEV) has become a useful tool in the field of neurochemistry and neuropharmacology for the analysis of the transport kinetics of dopamine (DA) and cocaine's mechanism of inhibition of DA transport in tissue homogenates [1–5]. The real-time uptake and efflux of catecholamines by transporters expressed in mammalian cells can also be monitored using RDEV [6, 7]. The application of RDEV to study transporter kinetics and mechanism in transporters expressed in cell lines using a single rotating electrode and then a double electrode configuration is described here, and several examples are given. Any substrate with a catechol functionality is easily oxidized and those with a single hydroxyl group are also oxidizable, although at a higher potential, at the glassy carbon rotating disk electrode (RDE). A catecholamine neurotransmitter of particular interest is DA, which is oxidized at the electrode to form the quinone (Scheme 1):



Scheme 1.

The RDE continuously generates an oxidation current that is proportional to the concentration of the substrate in the extracellular medium. Therefore, as uptake or efflux proceeds, the change in substrate concentration in the extracellular medium is measured. Figure 1 is a schematic of the RDE experimental apparatus. Approximately 2 million cells in solution are introduced into the electrochemical cell. The working electrode is concentrically rotated in the solution (4000 rpm), creating con-

vection paths flowing perpendicular to the electrode and then radially out from the surface. This rapid mixing of the cell or tissue suspension enables constant replenishment of the detected species to the electrode surface and minimizes the effects of diffusion on transport measurements. A potential is applied relative to an Ag/AgCl reference electrode while a Pt wire serves as an auxiliary electrode. In general for the RDE, the limiting current,  $I_L$ , produced by the oxidation or reduction of electroactive species at the electrode surface can be described by the Levich equation [8]:

$$I_L = 0.62 n F A C D^{2/3} \nu^{-1/6} \omega^{1/2}$$

where  $I_L$  is in mA,  $n$  is the number of electrons transferred per molecule,  $F$  is Faraday's constant (96,487 C/mol  $e^-$ ),  $A$  is the

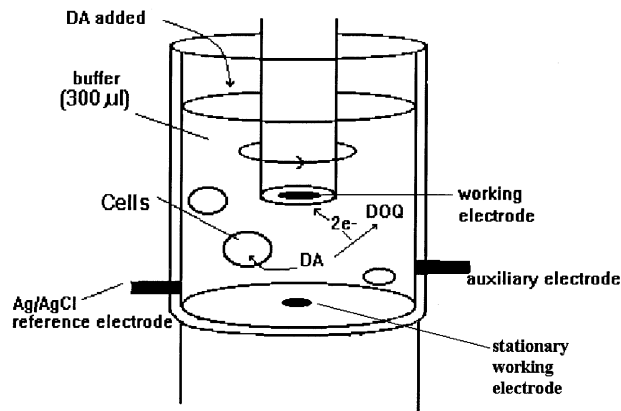


Fig 1. The experimental apparatus. The working electrode is rotated at 4000 rpm and the potential is held at +450mV (vs. Ag/AgCl). A second stationary electrode is positioned at the bottom face of the electrochemical cell and the potential is held at +650mV (vs. Ag/AgCl).

electrode surface area ( $\text{cm}^2$ ),  $C$  is the analyte concentration ( $\text{mmol}/\text{cm}^3$ ),  $D$  is the analyte diffusion coefficient ( $\text{cm}^2/\text{s}$ ),  $\nu$  is the kinematic viscosity of the solution ( $\text{cm}^2/\text{s}$ ), and  $\omega$  is the angular velocity of the rotating disk ( $\text{s}^{-1}$ ). With all parameters held constant in this equation, RDEV can be used for the purpose of monitoring the changing concentration of transporter substrate during uptake and efflux.

As seen in Figure 1, a second stationary electrode can be fitted to the bottom face of the electrochemical cell. The applied potential at this electrode can be held higher than that at the rotating electrode to allow for oxidation and subsequent monitoring of single and double hydroxyl substrates simultaneously with the recording of catechol oxidation at the rotating electrode.

The plasma membrane catecholamine transporters are integral membrane proteins whose function is to clear neurotransmitter from the extracellular fluid, thereby terminating synaptic transmission. The transport of DA and norepinephrine (NE) are of particular interest due to the fact that the dopamine transporter (DAT) is a site of action of many drugs of abuse, including cocaine and amphetamine [9], while some inhibitors of the re-uptake of NE at the norepinephrine transporter (NET), including desipramine, imipramine, and trimipramine [10, 11], have been effective in managing depression. The NET and DAT share a high degree of sequence homology [12, 13]. They are thought to possess 12 transmembrane spanning domains and are characterized by their cotransport of  $\text{Na}^+$  and  $\text{Cl}^-$  with substrate [10].

The work presented here involves examining the kinetics of a number of substrates at the human NET (hNET) expressed stably in LLC cells and transiently in COS cells using the RDE. In single electrode experiments, DA uptake is measured directly at the rotating electrode while the transport of *meta*-tyramine (*m*-TYR) and *para*-tyramine (*p*-TYR), single hydroxyl DA analogs is inferred indirectly through their induced efflux of DA. The effects of varying the concentration of preloaded DA and varying the concentration of tyramine used to induce efflux on initial rates of uptake and efflux of DA are examined. The use of two electrodes, one stationary and one rotating, to determine tyramine uptake simultaneously with DA efflux and thereby further define the kinetics of substrate transport at wild-type and mutant hNETs is also described.

## 2. Experimental

Dopamine hydrochloride was obtained from Sigma Chemical Co. (St. Louis, MO). *m*-Tyramine and *p*-tyramine were from Research Biochemicals International (Natick, MA). The LLC-NET cells and hNET cDNA in pcDNA3 vector were a gift from Dr. Randy Blakely (Department of Pharmacology, Vanderbilt University, Nashville, TN).

### 2.1. Apparatus

Rotating disk voltammetric measurements were made using a 3 mm diameter glassy carbon working electrode driven by an AFMSRX Analytical Rotator System (Pine Instrument Company, Grove City, PA). The electrochemical cell was equipped with a Pt auxiliary electrode and an Ag/AgCl reference electrode. An LC-4 amperometric detector (Bioanalytical Systems, Lafayette, IN) served as the potentiostat and the output current was amplified by a Keithley Model 427 amplifier (Keithley Instruments, Cleveland, OH). For the dual electrode studies, a modified cell was used

which contained a second stationary GCE Teflon shrouded glassy carbon electrode (2 mm diameter, Bioanalytical Systems, West Lafayette, IN) at the bottom of the cell. An Ensmann Instrumentation EI-400 (Bloomington, IN) served as the dual potentiostat and amplifier for this cell. For all experiments, the electrode was rotated at 4000 rpm and the temperature of the electrochemical cell was maintained at  $37^\circ\text{C}$ . The anodic currents were collected at a rate of 256 points per second by Origin 4.0 data acquisition software (Microcal Software, Northhampton, MA), averaged into 4 points per second, and plotted as a function of time. Origin 4.0 controlled the data collection via a Data Translation (Marlboro, MA) DT-2801 data acquisition board.

### 2.2. Cell Culture

COS cells were grown to confluence on  $150 \times 25$  mm petri dishes in Dulbecco's modification of Eagle's medium supplemented with 10% fetal bovine serum, 2 mM L-glutamine, and 10 000 units/mL penicillin/streptomycin and maintained at  $37^\circ\text{C}$  in a 5%  $\text{CO}_2$ , water-jacketed incubator. LLC-cells were grown in Eagle Minimum Essentials Medium with the above mentioned supplements. COS cells were transfected with 30  $\mu\text{g}$  of pcDNA3hNET or mutants by the calcium phosphate method [14]. DNA (30  $\mu\text{g}$ ) was dissolved in 675  $\mu\text{L}$  HPLC-grade  $\text{H}_2\text{O}$  and 75  $\mu\text{L}$  of a 2.5 M  $\text{CaCl}_2$  solution was added. 750  $\mu\text{L}$  of 2X HEPES-buffered saline (280 mM NaCl, 10 mM KCl, 1.5 mM  $\text{Na}_2\text{HPO}_4$ , 12 mM dextrose, 50 mM HEPES) was placed in a sterile conical tube. While bubbling air through the 2X HeBS, the DNA/ $\text{CaCl}_2$  solution was added dropwise to it. The mixture was vortexed, allowed to sit at room temperature for 20 minutes, and then added dropwise to a dish of cells. After 13 h of standard incubation, the medium was replaced and the cells were allowed to express the plasmid for 2 days.

### 2.3. Induced Efflux Experiment at one Electrode

LLC-NET or COS cells expressing the hNET were assayed for their ability to transport DA as follows. The cell medium was aspirated from the dish of cells and they were washed with 10 mL room temperature Krebs-Ringer-HEPES (KRH) (120mM NaCl, 4.7mM KCl, 2.2mM  $\text{CaCl}_2$ , 1.2mM  $\text{MgSO}_4$ , 1.2mM  $\text{KH}_2\text{PO}_4$ , 10mM HEPES, 10 mM D-glucose, pH to 7.4) buffer. The cells were scraped from a 150 mm  $\times$  20 mm dish with two 2.5 mL additions of KRH and then centrifuged at  $1000 \times g$  for 2 minutes. The supernatant was aspirated from the resulting pellet, 200  $\mu\text{L}$  of new KRH buffer was added to the COS cells and the suspension was transferred to the electrochemical cell. For the LLC cells, 1200  $\mu\text{L}$  of KRH buffer was added and a 300  $\mu\text{L}$  aliquot was introduced to the electrochemical cell. The remaining suspension was placed in a  $37^\circ\text{C}$  water bath for future assays. The electrochemical cell was equipped with a Ag/AgCl reference electrode and a Pt auxiliary electrode. The working electrode was polished with  $\gamma$ -alumina prior to each assay. To begin recording, the cell was raised so that the working electrode was positioned just below the surface of the solution. The working electrode rotation was started and a potential of 450 mV (vs. the Ag/AgCl reference electrode) was applied. After ample time for stable baseline acquisition, 6  $\mu\text{L}$  of DA dissolved in unbuffered electrolyte solution, KR, was added and the resulting oxidation current monitored. DA uptake into the cells via the transporter proceeded and a steady state was reached. An aliquot of *m*-TYR

or *p*-TYR was then added to induce the efflux of DA. For the transient expression systems, a negative control experiment was also performed by adding 6  $\mu\text{L}$  of DA to nontransfected COS cells. No uptake was observed in these nontransfected cells. Protein content for each assay was assessed using Biorad DC protein assay (Hercules, CA) with bovine serum albumin as the standard. Cell counting was performed using a hemocytometer.

#### 2.4. Data Analysis for one Electrode Experiment

Baseline current from ten seconds before DA addition was first subtracted from a current vs. time record. A linear regression was then performed on the uptake profile using an interval of 10–15 s beginning one second after the point of maximum increase in oxidative current. The length of time included in each regression analysis was dependent on the value of  $r^2$  ( $r^2 > 0.99$ ). The data were then converted to concentration vs. time using a calibration factor obtained by extrapolating the regression line back to the time of addition of DA. Using the calibration factor and the slope of the regression line, the initial rate of uptake was calculated. For efflux rate determination, a linear regression of the 30 s of baseline current, after DA has reached steady state, prior to tyramine addition was used for baseline subtraction. The initial rate of DA efflux was then determined from the slope of a regression line fit to the first 15–25 s of data following the addition of the efflux agent, which is not detected at an applied potential of 450 mV.

#### 2.5. Induced Efflux Experiment Using two Electrodes

The transport assay protocol was the same as that used when only one electrode was employed with a few exceptions. A dual potentiostat was used to control the potential of 400 mV applied

at the rotating electrode and 650 mV applied at the second stationary electrode fitted at the bottom face of the electrochemical cell. The higher potential applied at the second electrode allowed for oxidation of *m*-TYR in addition to oxidation of DA. The DA oxidative current was monitored at each electrode at the addition of DA alone and therefore the signal response at each electrode for a single concentration of DA could be calculated. Upon addition of *m*-TYR to induce efflux, the increase in oxidative current at the 650 mV electrode was used to calculate the signal response for the *m*-TYR concentration, as described below.

The data for the two electrode experiment was analyzed as described previously [15]. The increase in oxidative current at the 400 mV electrode corresponded to solely DA efflux while the change in current at the 650 mV electrode corresponded to changes in medium concentrations of DA and *m*-TYR from DA efflux and *m*-TYR uptake. The currents at the two electrodes were calibrated to initial added DA concentration as described for the one electrode experiment. The timecourse of DA concentration at the 400 mV electrode was then scaled by the relative response to DA at the two electrodes and subtracted from the calibrated signal at the 650 mV electrode to give the timecourse of the signal corresponding to *m*-TYR concentration. The *m*-TYR signal was then converted to *m*-TYR concentration over the *m*-TYR timecourse via the signal response factor for *m*-TYR at the 650 mV electrode. A linear regression was performed on the *m*-TYR concentration profile over the 15 s following the addition of *m*-TYR to obtain the initial rate of *m*-TYR uptake.

### 3. Results and Discussion

The timecourse of uptake of 1  $\mu\text{M}$  DA by the LLC-NET cells is depicted on the left panel of Figure 2. The decrease in DA

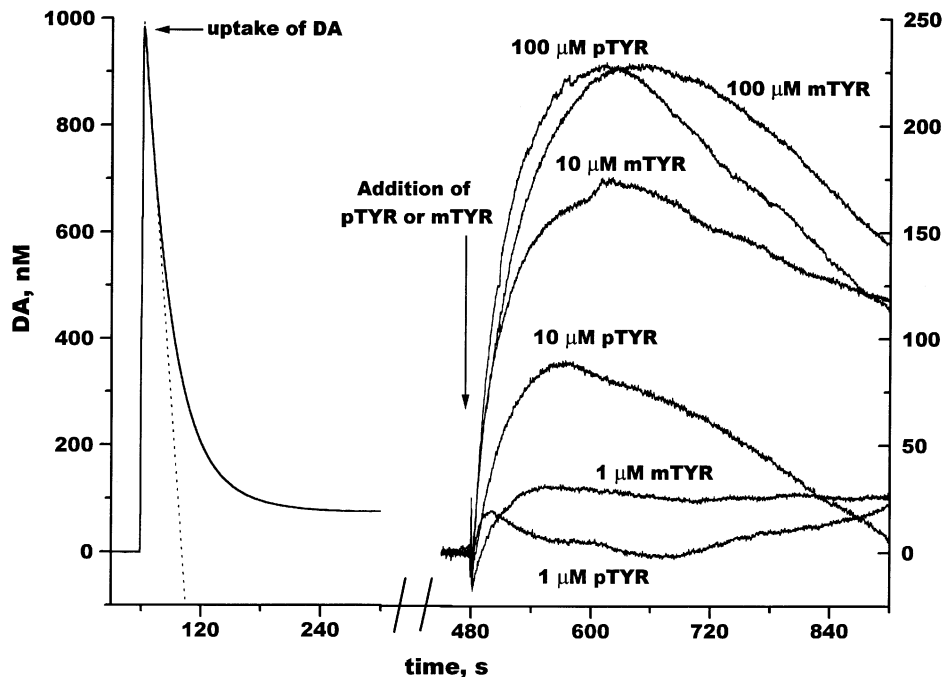


Fig 2. The effect of varying the concentration of *m*- or *p*-TYR on the initial rate of efflux of preloaded DA at LLC-NET cells. 1  $\mu\text{M}$  DA was added. Uptake occurred, and steady state DA level of approximately 100 nM is reached. The concentration of *m*- or *p*-TYR added to induce efflux varied logarithmically from 1 to 100  $\mu\text{M}$ . The curve label denotes the concentration of tyramine added and the arrows indicate the addition of DA and tyramine.

concentration in the extracellular medium is linear with respect to time for the first seconds of uptake, demonstrating essentially unidirectional transport. The initial rate of substrate uptake can be determined from the slope of a regression line fit to this region (dotted line in Fig.2). The Michaelis-Menten function:

$$v_o = (V_{\max} \times [S]) / (K_m + [S])$$

can be fit to initial rates of uptake from a range of added DA concentrations to obtain the kinetic parameters,  $K_m$  and  $V_{\max}$ , that characterize a substrate-carrier system.

Once the uptake of 1  $\mu\text{M}$  DA reached a steady state (Fig. 2), varying concentrations of *m*-TYR or *p*-TYR were added to the suspension to induce the efflux of DA by competing for the transporter at the external face of the cell membrane. At the 450mV applied potential, the transport of tyramine is not observed but its ability to stimulate efflux of DA demonstrates that it as well is transported by the hNET. However, it should be noted that not all efflux is transporter mediated [7]. Monitoring induced efflux extends the use of RDEV to study the transport properties of substrates not oxidized at the applied potential as well as different properties of the electroactive substrates. A possible mechanism and the timecourse of efflux is discussed elsewhere [16], but it is thought that the competition of tyramine for the transporter reduces the rate of inward transport of DA and increases the outward efflux of DA by driving the transporter to the inward facing conformation where it can bind DA. A net outward flux of DA occurs and is observed as an increase in external concentration of DA (Fig.2). As tyramine accumulates inside the cell, it begins to also compete with DA for binding to the inward facing empty transporter and DA efflux decreases. At the same time, DA concentration in the extracellular medium is increasing and competing more effectively with tyramine for the transporter, which causes an increase in inward flux of DA. When

the increasing inward flux of DA is equal to the decreasing outward flux of DA, a maximum in external concentration of DA is reached. Beyond that, net DA transport continues to be driven by the  $\text{Na}^+$  gradient inward as the system approaches a new steady state.

The effect of varying the concentration of *m*- and *p*-TYR on initial rates of DA efflux was first investigated (Fig. 2). The timecourses show both an initial rise and a maximum peak. The initial rates of efflux are expressed as a percentage of the initial rate of uptake of DA for each assay to normalize the data for the number of cells and level of transporter expression in each assay. The ratios of DA efflux/DA uptake for 1, 10, and 100  $\mu\text{M}$  *m*-TYR induced efflux were  $9.5 \pm 2.9\%$  ( $n = 3$ ),  $19.9 \pm 3.3\%$  ( $n = 4$ ), and  $25.8 \pm 2.4\%$  ( $n = 4$ ), respectively. For 1, 10, and 100  $\mu\text{M}$  *p*-TYR, the ratios were  $4.2 \pm .3\%$  ( $n = 4$ ),  $13.5 \pm 2.6\%$  ( $n = 3$ ), and  $19.9 \pm 1.0\%$  ( $n = 4$ ), respectively. The data show an increase in initial rate of efflux with increasing concentrations of added tyramine. The DA efflux rate is indicative of the relative transport rate of the substrate used to induce efflux.

The effect of varying the concentration of preloaded DA on initial rates of efflux using a single concentration of added tyramine to induce efflux was also examined (Fig. 3). DA concentration was varied from 0.5 to 2.5  $\mu\text{M}$ , and 100  $\mu\text{M}$  *p*-TYR was used to induce efflux. As the concentration of DA added increased, DA concentration in the medium approached steady state more slowly while the initial rate of uptake increased (for DA Michaelis-Menten kinetics, see [6]). Also, the external concentration of DA at equilibrium increased with increasing concentrations of added DA. It can also be seen that as the concentration of preloaded DA was increased, DA efflux increased. The DA efflux/uptake ratio increased from  $17.4 \pm 3.0\%$  at 0.5  $\mu\text{M}$  DA ( $n = 4$ ) to  $43.8 \pm 2.2\%$  at 2.5  $\mu\text{M}$  DA ( $n = 3$ ). The timecourse of induced DA efflux seen here is

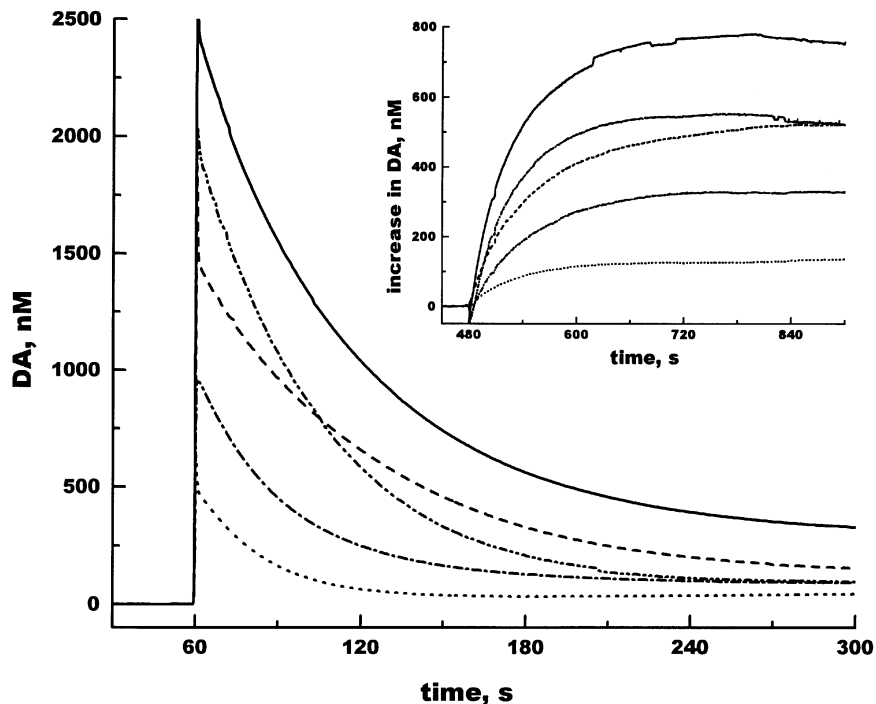


Fig 3. The effect of varying the concentration of preloaded DA on the initial rate of efflux of DA induced by a single concentration of *p*-TYR in LLC-NET cells. The timecourses for the uptake of DA represent the added concentrations of 0.5  $\mu\text{M}$  ( $n = 4$ ), 1.0  $\mu\text{M}$  ( $n = 114$ ), 1.5  $\mu\text{M}$  ( $n = 4$ ), 2.0  $\mu\text{M}$  ( $n = 4$ ), and 2.5  $\mu\text{M}$  ( $n = 4$ ). (Inset) The mean timecourses for the efflux induced by 100  $\mu\text{M}$  *p*-TYR on preloaded DA at the above mentioned concentrations.

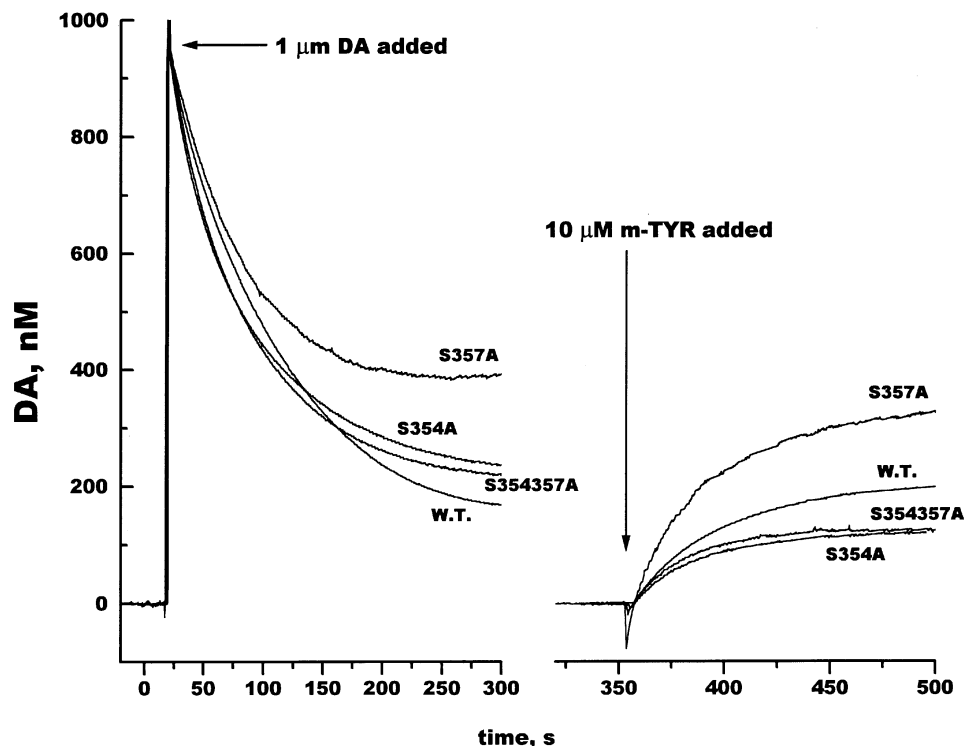


Fig 4. An example of the timecourse of 1  $\mu\text{M}$  DA uptake and efflux at wild-type and mutant transporters. DA efflux was induced by 10  $\mu\text{M}$  *m*-TYR and is plotted as an increase from steady state.

dependent on both the structure of the compound used to induce efflux as well as the concentration of both the preloaded DA and the efflux-inducing compounds. Interestingly, it can be shown that the ratio of the rate of induced efflux to the rate of uptake of efflux-inducing substrate is dependent only on the concentration of preloaded substrate [MS in preparation].

A particularly useful application of RDE is the combination of structural variation in substrates with structural variation in the transporter via site-directed mutagenesis. For example, to further define the role of the hydroxyl groups of the serine residues in transmembrane domain seven in the transport process, two amino acids in the hNET, serines 354 and 357, were substituted to alanine, singly and simultaneously, (S354A, S357A, and S354357A) [17]. These serines were investigated because analogous serines in the  $\beta$ -adrenergic receptor have shown to interact with ligands [18]. The transport of DA, and *m*- and *p*-TYR were examined at these mutant transporters using the induced efflux experiment. Typical concentration timecourse curves are shown in Figure 4. Absolute initial rates of uptake of 1  $\mu\text{M}$  DA and rates of efflux induced by 10  $\mu\text{M}$  *m*-TYR are shown as bar graphs in Figure 5. It is apparent that the efflux of DA is very different at the S357A and S354A mutant transporters. The absolute efflux rate at S357A is approximately five times higher than that at S354A. The observed difference is not due to a difference in levels of transporter expression as the  $V_{\text{max}}$  for DA uptake was not different for the two mutants [17]. What is not apparent in these results, however, is whether the difference in rates of efflux of DA seen at the mutants was due to a difference in *m*-TYR uptake or DA efflux, both inherent in these data. The efflux curve is the combined response to the uptake of tyramine and efflux or outward transport of DA. In order to determine whether the difference in induced efflux observed at mutants S354A and S357A was due to a difference in *m*-TYR uptake (not observed at the 450mV applied potential) or DA efflux or a combination of

both, the experiment was repeated using two working electrodes at different potentials. An example of the timecourse of the experiment is shown in Figure 6. The top panels (A and B) show

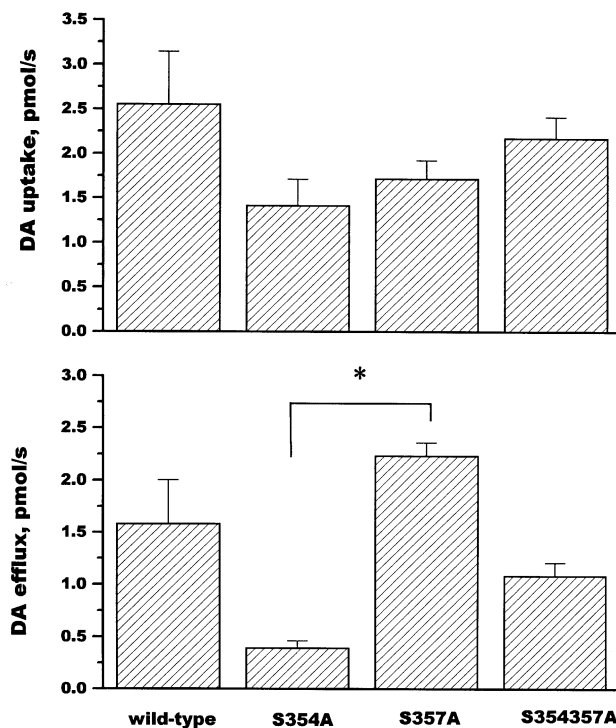


Fig 5. The absolute rates of uptake and efflux of 1  $\mu\text{M}$  DA at the wild-type and mutant transporters. DA efflux was initiated by 10  $\mu\text{M}$  *m*-TYR. The bar graphs are mean initial rates  $\pm$  SEM ( $n = 8-10$ ). \*:  $P < 0.05$  (*t*-test).

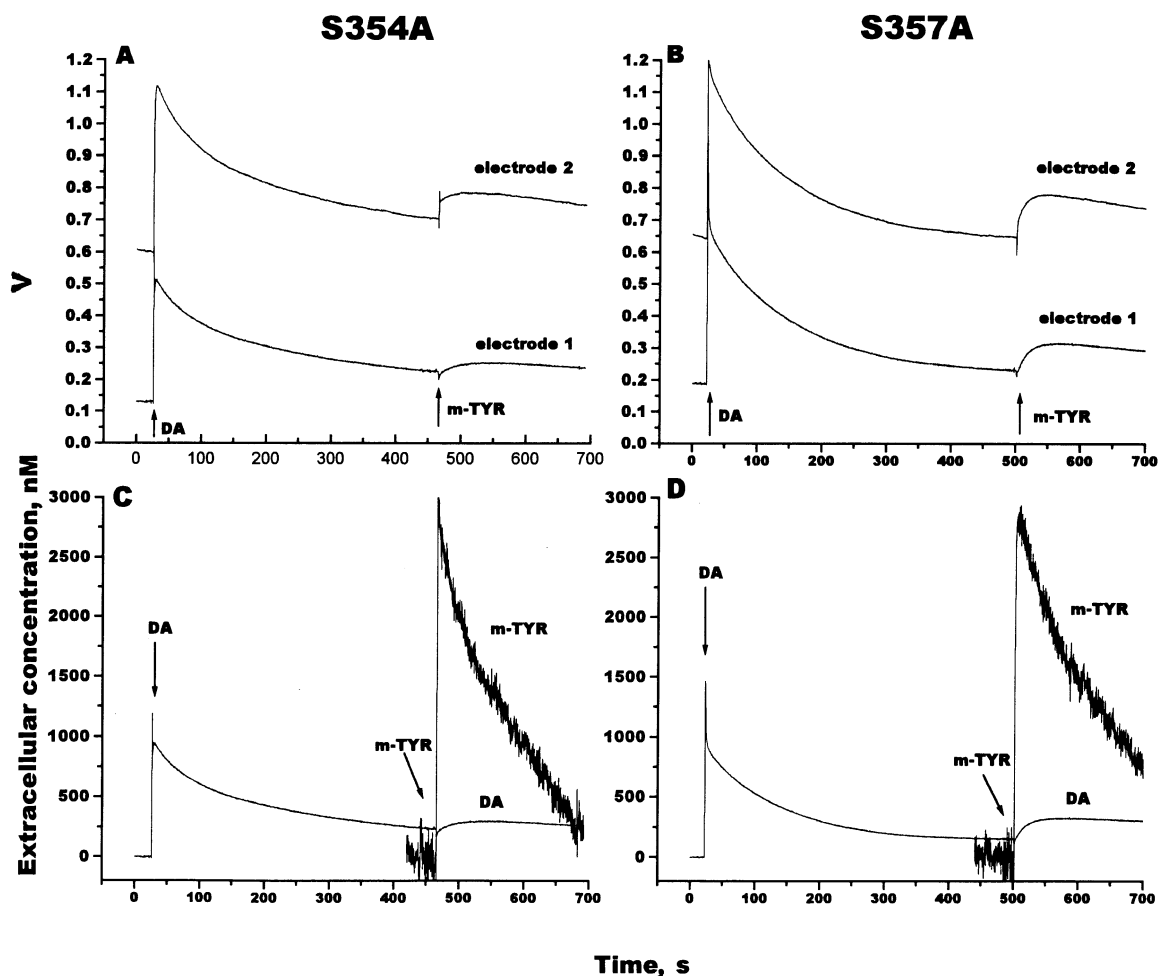


Fig 6. The simultaneous measurement of *m*-TYR uptake and DA efflux at the S354A and S357A mutant hNET transporters using a double electrode configuration. 1  $\mu$ M DA uptake proceeded until the extracellular DA concentration reached steady state. 3  $\mu$ M *m*-TYR was then added to induce spontaneous DA efflux. The arrows denote the addition time of DA or *m*-TYR. A) and B) show the oxidative signal of DA uptake and efflux and *m*-TYR uptake at the denoted mutant transporter where electrode 1 (450mV vs. Ag/AgCl) recorded the response to DA and electrode 2 (650mV vs. Ag/AgCl) recorded the response to *m*-TYR and DA. C) and D) show the changing extracellular DA and *m*-TYR concentrations over the timecourse of the experiment determined by subtracting the DA signal from the mixed DA and *m*-TYR signal at electrode 2, as described in the methods.

the oxidative signal for DA at electrode 1, and the sum of DA and *m*-TYR at electrode 2 at the two mutants, S354A and S357A. The lower panels (C and D) show the changes in extracellular concentration of DA or *m*-TYR versus time. The uptake of 3  $\mu$ M *m*-TYR is similar at both mutant transporters. However, it appears that the outward transport or efflux of DA is greater at S357A than at S354A.

This study demonstrates how a two electrode configuration can be applied to further extend the use of voltammetry to monitor the transport kinetics of two substrates simultaneously at the hNET. The data also provide information about the number of molecules of DA that are transported out relative to the number of *m*-TYR molecules transported in under these conditions. The ratio of the rate of DA transported out (pmol/s) to the rate of *m*-TYR transported in is equal to the number of molecules exchanged per unit time across the transporter. In this particular example, for S354A, for every one molecule of DA transported out, there were 7 molecules of *m*-TYR transported in (1.1 pmol/s : 8.1 pmol/s), and for S357A, for every two molecules of DA transported out, there were approximately 3 molecules of *m*-TYR transported in (2.0 pmol/s : 3.3 pmol/s). The difference in these ratios indicates that the mutation of serines 354 and 357 are

affecting the transporter very differently. It is expected that voltammetric observation of uptake and efflux, combined with site directed mutagenesis and other molecular biological approaches, will provide novel insights into catecholamine transporter kinetics and mechanisms.

#### 4. Acknowledgements

This work was supported by NIDA grant R03-DA10896. JBJ is a recipient of Research Scientist Award K02-DA00179.

#### 5. References

- [1] J.S. McElvain, J.O. Schenk, *Biochem. Pharmacol.* **1992**, *43*, 2189.
- [2] S.M. Meiergerd, S.M. Hooks, J.O. Schenk, *J. Neurochem.* **1994**, *63*, 1277.
- [3] S.M. Meiergerd, J.O. Schenk, *J. Neurochem.* **1994**, *63*, 1683.
- [4] S.M. Meiergerd, J.S. McElvain, J.O. Schenk, *Biochem. Pharmacol.* **1994**, *47*, 1627.
- [5] S.L. Povlock, J.O. Schenk, *J. Neurochem.* **1997**, *69*, 1093.

- [6] W.B. Burnette, M.D. Bailey, S. Kukoyi, R.D. Blakely, C.G. Trowbridge, J.B. Justice, Jr., *Anal. Chem.* **1996**, *68*, 2932.
- [7] N.H. Chen, G.C. Trowbridge, J.B. Justice, Jr., *J. Neurochem.* **1998**, *71*, 653.
- [8] Y.V. Pleskov, V.Y. Fillinovski, *The Rotating Disk Electrode*, Plenum Press, New York **1976**.
- [9] W.E. Bunney, Jr., J.M. Davis, *Arch. Gen. Psychiatry* **1965**, *13*, 509.
- [10] S.G. Amara, M.J. Kuhar, *Annu. Rev. Neurosci.* **1993**, *16*, 73.
- [11] L.L. Iverson, *Handbook of Psychopharmacology* (Eds: L.L. Iverson, S.D. Iverson, S.H. Snyder), Plenum Press, New York **1975**.
- [12] T. Pacholczyk, R.D. Blakely, S.G. Amara, *Nature* **1991**, *350*, 350.
- [13] B. Giros, S. El Mestikawy, N. Godinot, K. Zheng, H.Han, T. Yang-Feng, M.G. Caron, *Mol. Pharmacol.* **1992**, *42*, 383.
- [14] C.A. Chen, H. Okayama, *BioTechniques* **1988**, *6*, 632.
- [15] J.B. Justice, Jr., B. Reed, *Soc. Neurosci. Abstr.* **1997**, *23*, 695.
- [16] K.S. Danek, J.B. Justice, Jr., *Methods in Enzymology: Neurotransmitter Transporters* (Ed: S.G. Amara), Academic Press, San Diego, CA **1998**, pp. 649–660.
- [17] K.S. Danek Burgess, J.B. Justice, Jr., *J. Neurochem* **1999**, in press.
- [18] C.D. Strader, M.R. Candelore, W.S. Hill, I.S. Sigal, R.A.F. Dixon, *J. Biol. Chem.* **1989**, *264*, 13572.